Optical Engineering

SPIEDigitalLibrary.org/oe

Technical improvements applied to a double-pass setup for performance and cost optimization

Ferran Sanabria
Mikel Aldaba Arévalo
Fernando Díaz-Doutón
Carlos Enrique García-Guerra
Jaume Pujol Ramo

SPIE

Technical improvements applied to a double-pass setup for performance and cost optimization

Ferran Sanabria,* Mikel Aldaba Arévalo, Fernando Díaz-Doutón, Carlos Enrique García-Guerra, and Jaume Pujol Ramo
Universitat Politècnica de Catalunya, Center for Sensors, Instruments and Systems Development (CD6), Rambla Sant Nebridi 10, 08222 Terrassa, Barcelona, Spain

Abstract. We have studied the possibility of improving the performance, simplifying, and reducing the cost of a double-pass system by the use of alternative technologies. The system for correcting the spherical correction has been based on a focusable electro-optical lens, and a recording device based on CMOS technology and a superluminescent diode (SLED) light source have been evaluated separately. The suitability of the CMOS camera has been demonstrated, while the SLED could not break the speckle by itself. The final experimental setup, consisting of a CMOS camera and a laser diode, has been compared with a commercial double-pass system, proving its usefulness for ocular optical quality and scattering measurements. © *2014 Society of Photo-Optical Instrumentation Engineers (SPIE)* [DOI: 10.1117/1.OE.53.6.061710]

Keywords: electro-optical liquid lens; tunable lens; optical quality; eye refraction; superluminescent diode; laser diode; double-pass; scattering.

Paper 131161SS received Jul. 31, 2013; revised manuscript received Jan. 28, 2014; accepted for publication Feb. 11, 2014; published online Mar. 10, 2014.

1 Introduction

The double-pass technique is based on projecting a point source on the retina and recording images after retinal reflection and double-pass through the ocular media.[1] This technique has shown its usefulness for the evaluation of the optical quality[2,3] and also the scattering of the eye.[4,5] It has been widely used in physiological optics studies to assess different aspects of the eye as age related changes in the optical quality,[6] the depth of field,[7] or accommodation.[8–10] Moreover, there is a commercial instrument based on the double-pass technique[11] which has given rise to works more focused on the daily clinical practice, such as the comparison between refractive surgery and intraocular lenses implantation,[12] the effect of refractive surgery on vision analyzed using preoperative optical quality,[13] comparison between refractive surgery techniques,[14] evaluation of intraocular lenses,[15] the study of the optical quality after corneal transplantation,[16] in retinal pathologies,[17] grading cataracts using an objective index,[18] or tear-film quality dynamic measurements.[19]

In Fig. 1, a schematic representation of a double-pass setup is shown, including the most important components: a punctual light source, a Badal system to correct the spherical refraction, two diaphragms that act as entry and exit pupils and a camera to record the images. The most common double-pass configuration includes a laser as light source, usually a laser diode (LD) with a near-infrared (NIR) wavelength (around 780 nm), a Badal system formed by two lenses with a variable distance between them, two diaphragms acting as pupils and a charged-coupled device (CCD) camera as recording device. This configuration is used on the commercial instrument based on the double-pass technique,[11] and similar configurations are also used for instance in Hartmann-Shack aberrometers,[20,21] including in this case, an array of microlenses placed before the CCD camera. But today, due to the growth of technology, there are different alternatives available to be used in this configuration, related mainly to the light source, the Badal system, and the camera. The use of these alternatives allows compacting the setup, obtaining faster measurements, and reducing the cost.

The Badal optometer is a system for spherical refraction correction consisting of two fixed lenses and two moving mirrors. The distance between the lenses is variable, so the optical path can be changed, thus compensating the spherical refraction of the system. The Badal system is simple and allows a wide range of spherical corrections. However, its weakness is the use of movable components, which makes the system slow and increases the setup dimensions. Recently, an alternative for spherical correction based on focusable electro-optical lenses (EOLL) has been proposed.[22] These lenses consist of an optical fluid covered by an elastic membrane. The curvature of the EOLL changes when a current is applied, modifying the spherical power of the lens. The use of the EOLL enables a fast spherical correction without movable components. It is also a compact subsystem which is easy to align and reduces the double-pass setup dimensions.

Regarding the light source, lasers[1,6] and LDs[8,9,11] have been used in double-pass systems. Their usefulness for optical quality measurement has been proved, but they show an important limitation due to their high coherence. This, combined with the diffusing properties of the retina, produces a speckle pattern in the recorded images. Several solutions have been proposed for reducing the speckle noise, such as the temporal integration[1] or the use of a scanning system to do a spatial average.[23] The use of a light source with lower coherence as a superluminescent diode (SLED) has also been proposed.[23] The SLEDs have been used to reduce speckle in

*Address all correspondence to: Ferran Sanabria, E-mail: ferran.sanabria@upc.edu

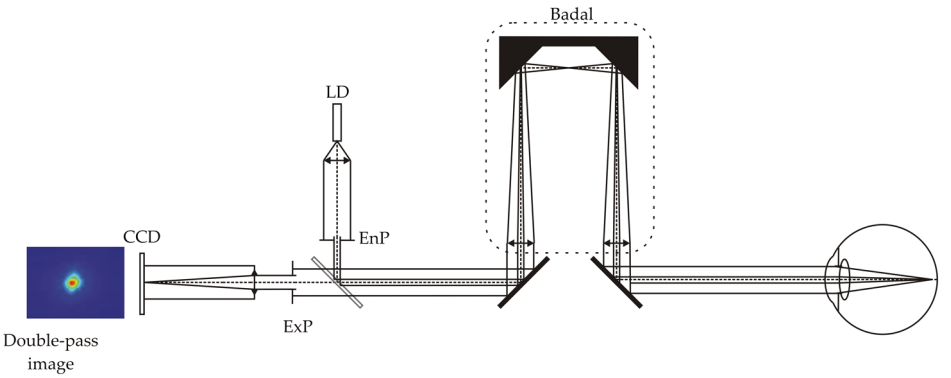

Fig. 1 Schematic representation of a double-pass setup. LD, laser diode; EnP, entrance pupil; ExP, exit pupil; CCD camera; Badal system; and DP image.

combination with scanning or with the use of quarter-wave plates[23] or alone.[24] The main problem of the SLEDs used to be the economical cost, but nowadays, due to the technological improvements, cheaper SLEDs can be found.

The CCD was invented in 1970 as a memory device, but since then the potential of technology has led it to become a sensor with an important development.[25] It is widely used in visual optics instrumentation, and specifically as a sensor to record double-pass images.[6,7,11] On the other hand, CMOS technology although born in the 1960s to 1970s was not competitive in relation to CCD until the 1990s.[26] CMOS technology has not been used so extensively in visual optics for image recording in double-pass or similar setups. In the last years, it has been used in fast Hartmann-Shack sensors[27] or in optical coherence tomography scanning,[28] although it is still not used as much as CCDs. This could be mainly due to the disadvantages that CMOS cameras have in comparison with CCD cameras, such as a poorer image quality, sensitivity, and, mainly, a higher level of noise.[26] On the other hand, it presents some advantages such as high speed of acquisition and lower price. The development in CMOS technology over the last few years has narrowed the differences with CCD cameras, and nowadays it could be an alternative in visual optics setups.

The purpose of this study was to develop a new double-pass configuration based on new technological improvements, in order to simplify the setup, improve its performance, and reduce costs. The system included an EOLL as the system to correct the spherical refraction, which simplified the setup. The suitability of a CMOS camera and a low-cost SLED to measure the optical quality and scattering in a double-pass system was evaluated. The results obtained with these technological improvements for optical quality measurements are not exclusive of the double-pass system and could be applied to similar techniques such as Hartmann-Shack based aberrometers.

2 Materials and Methods

2.1 *Instrumentation*

A custom-built double-pass setup with two light sources (LD and SLED) and two image recording devices (CCD and CMOS cameras) was used for the purpose of this work. A scheme of the setup is shown in Fig. 2. In the first pass, a point source is projected on the retina. The light source is an LD (Monocrom MC7805U-M-7A15, $\lambda = 780$ nm) or an SLED (Monocrom SLED-7810M-7G25, $\lambda = 780$ nm), with a full width at half maximum of 3 and 20 nm respectively, both collimated. The used SLED is four times cheaper than the conventional SLED models. The light coming from each source passes through a 2-mm diameter diaphragm (EP_1 and EP_2) acting as the entrance pupil of the system. The light coming from the SLED is transmitted through the BS_1 beam splitter while light coming from LD is reflected. Afterwards, the optical path for both light sources is identical. The light is reflected in a beam splitter (BS_2) and then in a hot mirror, fixed to a vibrating motor which enables speckle noise reduction.[23] Then the light passes through an EOLL is reflected in a mirror (M_1) and passes through a 50 mm focal length lens (L_1). A couple of lenses EOLL and L_1 act as a spherical compensator, being the distance between both lenses twice the focal of the L_1 lens. At the exit of the spherical compensator, the light is reflected in a dichroic filter, which reflects 780 nm and transmits the light with wavelengths larger than 850 nm,

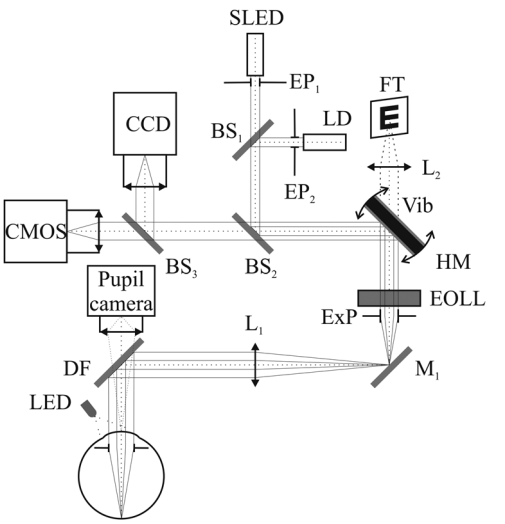

Fig. 2 Scheme of the experimental setup. LD: laser diode; SLED: superluminescent diode; L_1 and L_2: lens; EOLL: electro-optical liquid lens; M_1: mirror; BS_1, BS_2, and BS_3: beam splitters; DF: dichroic filter; HM: hot mirror; EP_1 and EP_2: entrance pupils; ExP: exit pupil; FT: fixation test; CCD, CMOS, camera pupil: CCD and CMOS cameras used for the double-pass measurements and pupil monitoring, respectively; LED: pupil illumination LEDs; and Vib: vibrating motor.

and reaches the eye. The distance from the L_1 lens to the eye is also twice the focal of the L_1 lens.

After retinal reflection, the second pass begins with an identical path to that of the first pass until BS_2. In the second pass, the light coming from the eye is limited by a 4 mm diaphragm (ExP) acting as exit pupil of the system and conjugated to the subject's pupil plane. Afterwards, the light coming from the retina is divided by means of a beam splitter (BS_3) in order to record images in both cameras (μeye UI-2220-M CCD and μeye UI-1220-M CMOS). The pixel size is $8.3(\mathrm{H}) \times 8.3(\mathrm{V})$ μm for CCD and $6(\mathrm{H}) \times 6(\mathrm{V})$ μm for CMOS cameras that corresponds to a frequency sampling of 0.821 and 1.136 cycles/deg, respectively. The pupil is illuminated with LEDs ($\lambda = 1050$ nm) and an additional web camera (pupil camera) is used for pupil monitoring and centering. A fixation test with a luminance of 20 cd/m^2 and collimated by means of a lens (L_2) is used for patients' correct alignment.

The main technical specifications of the recording devices, light sources, and EOLL are summarized in Table 1.

As mentioned above, the spherical compensator consisted on the couple of lenses L_1 and EOLL. We have used the commercial fast electrically tunable lens EL-10-30-NIR-LD (Optotune, Dietikon, Switzerland) with a focal range from +36 to +132 mm. The lens L_1 is introduced into the system in order to shift the focal range of the EOLL providing a range of spherical compensation from +10 to −10 diopters (D) at the pupil plane. Moreover, this lens (L_1) is used to ensure that the diaphragm acting as exit pupil (ExP) is conjugated with the pupil of the patient. The suitability of the EOLL as a spherical compensator has been demonstrated and the spherical compensator characterized in a previous study.[22] The errors due to curvature and consequent thickness changes in the EOLL when varying the focal length were studied in the mentioned work, concluding that are negligible when measuring the optical quality of the eye.

Regarding the image sensor, as previously reported, usually CMOS sensors have a higher level of noise. In our case, when measuring the noise level by means of the peak signal-to-noise ratio [$\mathrm{PSNR} = 20 \times \log(\mathrm{IMAX}/\sigma)$][29] where IMAX is the maximum possible value of the intensity [255] and σ is the standard deviation of the intensity values in the image, we obtained a value of 49.27 dB for the CCD and 47.15 dB for the CMOS sensor. The higher the PSNR, the lower the noise. Although the noise is higher for the CMOS than for the CCD, it represents <1% of the maximum possible intensity [255] in the image for both cameras. Regarding the prices of the sensors, the CMOS camera was between 2.5 and 3 times cheaper than the CCD camera.

In order to obtain the reference measurements, the commercial double-pass system optical quality analysis system (OQAS) (Visiometrics SL, Terrassa, Spain) was used.[11] The OQAS instrument works with an LD emitting at 780 nm as light source and a CCD camera as image recorder, with similar specifications to the components in our setup. To compare the results obtained by the optical quality was evaluated in terms of modulation transfer function cutoff ($\mathrm{MTF_{cutoff}}$), a metric directly related to visual acuity and commonly used in similar studies[13] and the scattering was evaluated by means of the Objective Scatter Index (OSI).[5] The $\mathrm{MTF_{cutoff}}$ is calculated as the frequency with an MTF

Table 1 Main technical specifications of the recording devices, light source, and EOLL.

	Recording devices	
	UI-2220-M CCD	UI-1220-M CMOS
Image sensor	1/2 in. CCD	1/3 in. CMOS
Resolution	768(h) × 582 (v) pixel, CCIR/PAL	752(h) × 480(v) pixel, WVGA
Pixel size	8.3(H) × 8.3(V) μm	6(H) × 6(V) μm
Color depth	8 bits	8 bits
	Light source	
	SLED-7810M-7G25	MC7805U-M-7A15
Wavelength (@20°C) (nm) ±20	780	780 ± 5
Po.max (mW)	1.9 mW	1.5 mW
Operation modes	Modulatable and CW	Modulatable and CW
Clear aperture	6.5 mm	7 mm
	EOLL (EL-10-30-NIR-LD)	
Clear aperture		10 mm
Control voltage		0 to 5 V
Power consumption		0 to 2 W
Focal tuning range @ 525 nm^2		+45 to +120 mm

value of 0.01. The MTF of the eye is obtained as the Fourier transform of the double-pass image divided by the diffraction limited MTF corresponding to a pupil diameter of 2 mm.[3] A high MTF_{cutoff} is usually related to a good optical quality and it is normally assumed that a cutoff frequency of 30 cycles/deg corresponds to a decimal visual acuity of 1.0. The parameter OSI is calculated as the ratio between the integrated light in a peripheral annular area (from 12 to 20 arc min) and the central peak (1 arc min) of the double-pass image divided by 10. Patients with low intraocular scattering have an OSI value below 1.[5]

2.2 *Subjects and Procedure*

Thirty-two healthy young adults (10 females and 22 males), recruited from the staff and students of the Centre for Sensors, Instruments and Systems Development (CD6) of the Universitat Politècnica de Catalunya participated in the study. All subjects gave their written informed consent after receiving a written and verbal explanation of the nature and the aims of the study. The research followed the tenets of the Declaration of Helsinki.

Criteria for inclusion were no history of any ocular pathology, surgery, and/or pharmacological treatment. Only subjects with a pupil diameter of 4 mm or more in scotopic conditions were included in the study, as this was the size used in the measurements performed with the double-pass system. Furthermore, subjects were included in the study if their refractive error (in terms of spherical equivalent) ranged from −8.00 to +5.00 D, since this is the measurement range for the OQAS instrument, and the astigmatic error is <0.50 D.

The mean age [±standard deviation (SD)] of the population was 37.21 ± 8.29 years (range 24 to 50). The mean spherical refractive error was -0.57 ± 1.87 D (range: +2.5 to −4.5 D. In terms of optical quality and scattering, the mean MTF_{cutoff} and OSI values obtained with the OQAS were 38.61 ± 8.25 cycles/deg and 0.54 ± 0.21, respectively.

Double-pass measurements were performed under low illumination conditions in order to guarantee pupils larger than 4 mm in all the cases. All examinations were performed by the same trained examiner. The eye that was measured (left or right) was randomly selected.

As has been previously said, the objective of this work has been the evaluation of a CMOS camera and a low-cost SLED to be used in a double-pass setup, and the proposal of a double-pass system based, if possible, on these components. With this aim, the following comparisons were performed:

1. CMOS camera: Double-pass images were simultaneously recorded from each patient with each of the cameras (CCD and CMOS). Six images were recorded with each sensor, with exposure time of 240 ms, and subtracting a background image. The results (MTF_{cutoff} and OSI) obtained when measuring with the CMOS camera were compared with the results from the CCD camera.
2. SLED: Double-pass images were recorded from each patient with each of the light sources (SLED and LD). When each of the light sources was used, the other source was switched off. As the goal of using an SLED source was to reduce the speckle noise and to avoid the use of a vibrating motor, measurements with the SLED were performed with the vibrating motor switched off, while when using the LD the motor was on. The results (MTF_{cutoff} and OSI) obtained when measuring with the SLED were compared with the results from the LD.
3. Experimental double-pass system: Depending on the results when evaluating the light source and the recording device, a final configuration was adopted. To demonstrate the suitability of this configuration, the results (MTF_{cutoff} and OSI) from the images for each patient taken with the experimental double-pass setup were compared with OQAS instrument results.

2.3 *Statistics*

Statistical analysis was performed using commercial SPSS software for Windows (version 17.0, SPSS, Chicago, Illinois). A p value of 0.05 was considered significant.

The Kolmogorov–Smirnov (K–S) test was used to evaluate the normal distribution of all variables analyzed, i.e., the MTF_{cutoff} and OSI values obtained by means of the double-pass images. The mean value (±SD) is given for each of them.

The validity of the SLED and CMOS camera as the ability to measure correctly the optical quality and scattering of the eye was tested from different points of views. First, the mean difference between the tested and conventional methods is given. In explanation, when evaluating the light source, we compute the mean difference between SLED and LD measurements, and when evaluating the recording device we calculate the mean difference between CCD and CMOS measurements. Second, the correlation coefficients were used in the same comparison. Pearson's correlation coefficient and its significance are given for each case. Finally, a paired sample t test was carried out to analyze if there were significant differences between the optical quality and scattering measurements reported by the tested and conventional methods.

The final configuration of the experimental setup was evaluated by comparison with the commercial instrument. The mean difference, the correlation, and the t test were also used. Moreover, a Bland and Altman analysis[30,31] was performed to study the agreement between setups. In this method, the difference between measurements is plotted against the mean value. The 95% confidence limits are calculated as 1.96 times the standard deviation of the mean difference. The Pearson correlation coefficient of the Bland and Altman graph was used to evaluate if there was any tendency in the differences to vary depending on the mean value of the measurements.

3 Results

3.1 *Suitability of a CMOS Camera*

In this study, the performance of the CMOS and CCD cameras for measuring the optical quality and scattering of the eye was compared. In Fig. 3, two double-pass images corresponding to the same patient recorded with a CMOS camera and a CCD camera are shown. As seen in Fig. 3, both images are very similar. The obtained results considering

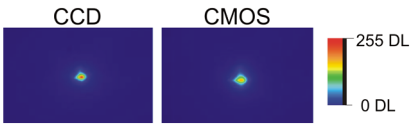

Fig. 3 Double-pass images for the same patient registered with CCD (left) and CMOS (right) cameras. (DL, digital level).

all the eyes measured are shown in Table 2. The mean differences between the CMOS and CCD cameras in terms of MTF_{cutoff} and OSI values were close to zero. The mean values of these parameters measured by the OQAS system were 38.61 ± 8.25 and 0.54 ± 0.21 cycles/deg, respectively, thus the difference between both cameras corresponds to an error of 2.31% and 2.21%. The existing correlation between the results corresponding to CMOS and CCD cameras for MTF_{cutoff} and OSI was also investigated. There was a significant correlation between data with Pearson correlation coefficients above 0.918 in both cases. Finally, after confirming the normal distribution of the values in all cases with the K–S test ($p > 0.05$), we compared the measurements obtained by each camera with the paired sample t test, and no significant differences were found between metrics ($p > 0.05$).

3.2 *Suitability of an SLED*

In this study, the performance of the SLED and LD light sources for measuring the optical quality and scattering of the eye was compared. In Fig. 4, an example of double-pass images for the same patient when using the LD and the SLED as light sources is shown. As seen in this figure, the image using the SLED shows the presence of residual speckle.

The mean differences between SLED and LD light sources in terms of MTF_{cutoff} and OSI values are shown in Table 2. As in a previous comparison, taking OQAS mean values as reference, the mean perceptual difference was of 7.08% and 2.76% for the MTF_{cutoff} and OSI. The existing correlation between the results corresponding to SLED and LD sources for MTF_{cutoff} and OSI was also investigated. As shown in Table 2, there was a significant correlation between data with Pearson correlation coefficients around 0.700 in both cases. Finally, after confirming the normal distribution of the values in all cases with the K–S test ($p > 0.05$), we compared the measurements obtained by each light source with the paired sample t test. No significant differences were found for OSI values, while statistically significant differences were found in the MTF_{cutoff} when comparing the results obtained with an SLED and LD (Table 2).

3.3 *Evaluation of the New Double-Pass Configuration*

Results obtained show that there are no differences between cameras and, therefore, the CMOS camera was used in the final configuration of the experimental setup. On the other hand, the low-cost SLED that we have used does not have sufficient bandwidth to break speckle by itself and consequently there are differences in the MTF_{cutoff}. Thus, in the final configuration of the experimental setup, the LD was used as light source. Moreover, the experimental setup included a spherical corrector based on an EOLL. The performance of the setup was compared with the commercial double-pass system OQAS.

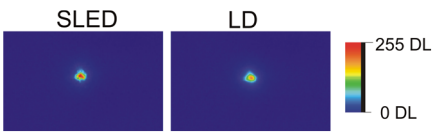

Fig. 4 Double-pass images for the same patient registered when using SLED (left) and LD (right) as light sources. (DL, digital level).

The mean differences between the experimental setup and the OQAS sources in terms of MTF_{cutoff} and OSI values were 1.14 ± 4.10 and -0.04 ± 0.16, respectively. Thus, the mean difference in terms of percentage is 2.93% for the MTF_{cutoff} and 7.55% for the OSI. The existing correlation between the results, shown in Fig. 5, highlighted a Pearson correlation coefficient of 0.873 ($p < 0.001$) and 0.783 ($p < 0.001$) for MTF_{cutoff} and OSI, respectively.

In the Bland and Altman analysis (Fig. 6), the differences for MTF_{cutoff} and OSI between setup and OQAS measurements are shown against the mean value, within the $\pm 1.96 \times$ SD range. No significant correlations were found in this case and therefore, we considered that there was no dependency of the difference between setups with the mean values [MTF_{cutoff}: $r = 0.05$ ($p = 0.776$) and OSI: $r = 0.32$ ($p = 0.073$)].

Finally, after confirming the normal distribution of the values in all cases with the K–S test ($p > 0.05$), we compared the measurements obtained with the experimental setup and the OQAS with the paired sample t test. No significant differences were found for MTF_{cutoff} values ($p = 0.126$), or for OSI values ($p = 0.161$).

4 Discussion

The current study evaluated the suitability of CMOS cameras and SLED light sources to be used in double-pass setups for measuring optical quality and scattering of the human eye, and which could also be adapted to other systems such as Hartmann-Shack based aberrometers. First, we studied the performance of a CMOS camera on a double-pass system by comparison with the results obtained with a CCD. Second, SLED light source was evaluated by comparison with an LD. Finally, the proposed experimental setup was compared with a commercially available double-pass system. All the tested setups included an EOLL as a system for correcting the spherical refraction. Therefore, we have checked the different technological alternatives that exist in the main parts of double-pass systems.

When comparing the optical quality (in terms of MTF_{cutoff}) and intraocular scattering (in terms of OSI) measured with the CMOS and CCD cameras, we found small differences between both methods. Moreover, we found a high Pearson correlation coefficient between the results obtained with both cameras and no statistically significant differences. With all these data, we can conclude that there are no differences between the CCD and CMOS cameras used in our study when measuring optical quality and intraocular scattering, and thus demonstrating the suitability of CMOS cameras for this purpose. This is consistent with the conclusion obtained for other techniques. For example, a previous work using the Hartmann-Shack technique,[27] where the noise is an important factor influencing the final result of the measured wavefront,[32] successfully used a CMOS

Table 2 Comparison of MTF_{cutoff} and OSI values when evaluating the CMOS (versus CCD) camera and the SLED (versus LD) light source. The mean difference (±SD) between pairs of metrics, the Pearson correlation coefficient and its significance *t*, and the paired sample *t* test results are shown.

	CMOS versus CCD		SLED versus LD	
	MTF_{cutoff}	OSI	MTF_{cutoff}	OSI
Mean difference ± SD	0.89 ± 3.18	0.01 ± 0.10	−2.73 ± 4.60	−0.01 ± 0.19
Pearson correlation coefficient, *r* (*p*)	0.920 (<0.001)	0.918 (<0.001)	0.759 (<0.001)	0.696 (<0.001)
Paired sample *t* test (*p*)	0.123[a]	0.500[a]	0.002	0.666[a]

[a]No significant differences.

camera as a recording device. Although traditionally, the CMOS cameras suffered from higher noise levels than CCD cameras, the sensors we have used in this work had a similar PSNR. This demonstrates the evolution of this type of sensors, and confirms their suitability for visual optics setups and instrumentation.

When comparing the SLED and LD measurements, we found a different behavior for the MTF_{cutoff} and OSI parameters. For the latter parameter, comparing the SLED with an LD, we found small differences in its numerical values, a high Pearson correlation coefficient and no statistically significant differences when applying the *t* test. Thus, from these data we could conclude that there are no differences in OSI results between LD and SLED measurements.

On the other hand, MTF_{cutoff} parameters highlighted a difference in its numerical values, a high Pearson correlation coefficient and statistically significant differences when applying the *t* test. The reason for this difference could be

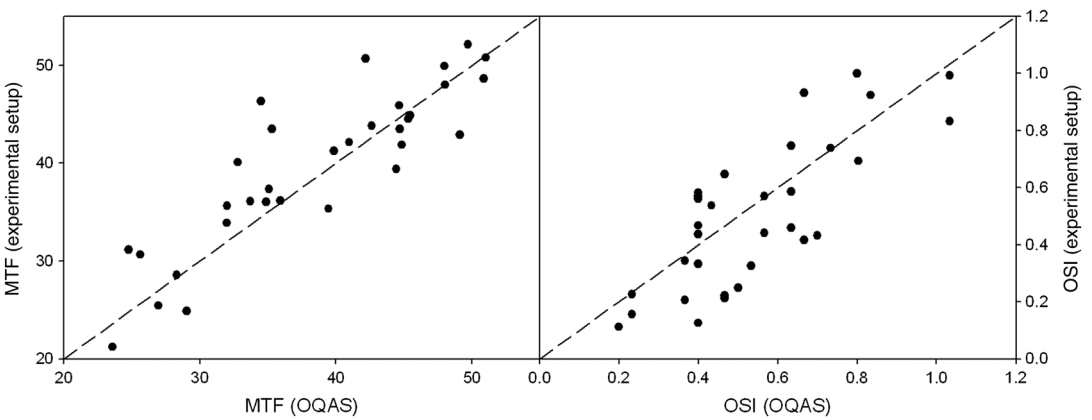

Fig. 5 Correlation of the MTF_{cutoff} and OSI values measured with the experimental setup and the OQAS instrument.

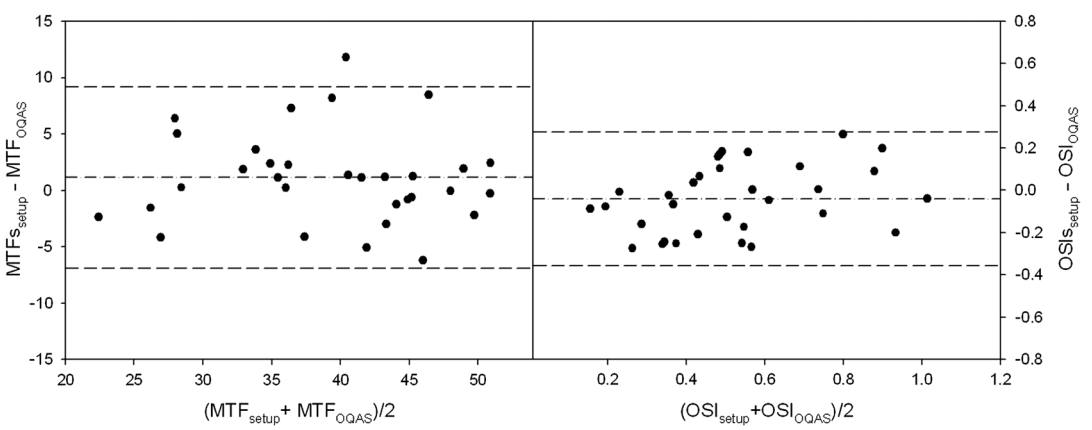

Fig. 6 Bland and Altman plots showing the mean values of the differences between the MTF_{cutoff} and OSI measurements and the 95% confidence limits (dashed line) when the experimental setup and OQAS instrument are compared.

due to the insufficient reduction of the speckle noise in the images recorded with this SLED. In this sense, we repeated the comparison between SLED and LD, but with the scanning motor switched on in both cases and found that there were no statistically significant differences between light sources either in the MTF_{cutoff} ($p = 0.533$) or in the OSI value ($p = 0.310$). Thus, in similar conditions (both light sources with the vibrating motor switched on) the performance of the LD and the SLED is the same, i.e., the optical quality measured with both devices is similar. Additionally, when comparing the SLED measurements with and without motor, we found statistically significant differences for the MTF_{cutoff} ($p = 0.001$), while no differences for the OSI value ($p = 0.549$) were found. The only difference between both cases (scanning motor switched on and off) is the speckle reduction, thus we can conclude that the speckle in the SLED images when the motor is switched off is affecting the MTF_{cutoff} calculation.

To analyze in more detail the effect of the speckle, it has been quantified by means of the widely used contrast of speckle (Cs) criteria.[33,34] For measuring the Cs, the image is divided in small windows and for each one, the ratio between the standard deviation of the intensities in the window and the average of the intensity is calculated. The Cs corresponds to the average of the ratio calculated for all the windows in the image. The Cs ranges from 0 (minimum speckle) to 1 (maximum speckle). The Cs value for the LD with the scanning motor on was of 0.12, while the Cs for the SLED with the scanning motor switched off was of 0.24 and with the scanning motor switched on was of 0.11. These data show that when using SLED with scanning motor switched off there is less reduction in the speckle than when using any of the light sources with the scanning motor switched on. Additionally, some previous works reported no problems with speckle noise when using the SLED as the only method for speckle reduction,[24] while other authors opted for combining it with other methods such as scanning motor and phase plates.[23] In our case, the used SLED did not have sufficiently low coherence to break the speckle noise on its own, but showed a good performance when being combined with other methods for speckle reduction. Thus, we can conclude that the SLED could be used in the absence of a vibrating motor if it had a slightly lower coherence.

After the evaluation of the light source and the recording device, the final configuration of the setup included the LD (with the vibrating motor) and the CMOS camera, and an EOLL as spherical corrector. When comparing the performance of the experimental setup with a widely used commercial device, all the tests (mean difference, Pearson correlation coefficient, and *t* test), showed the good agreement between both systems. Thus, we can conclude that the proposed experimental setup, including as innovations the CMOS camera and the EOLL spherical corrector, is comparable to the commercial device.

Acknowledgments

This study was funded by the Spanish Ministry of Science and Innovation with the project Grant No. DPI2011-30090-C02-01 and by the European Union. C. E. Garcia-Guerra thanks to the European Union for the Ph.D. grant he has received in the Erasmus Mundus Joint Doctorate Program Europhotonics.

References

1. J. Santamaría, P. Artal, and J. Bescos, "Determination of the point-spread function of human eyes using a hybrid optical-digital method," *J. Opt. Soc. Am. A* **4**(6), 1109–1114 (1987).
2. D. R. Williams et al., "Double-pass and interferometric measures of the optical quality of the eye," *J. Opt. Soc. Am. A* **11**(12), 3123–3135 (1994).
3. P. Artal et al., "Double-pass measurements of the retinal image quality with unequal entrance and exit pupil sizes and the reversibility of the eye's optical system," *J. Opt. Soc. Am. A* **12**(12), 2358–2366 (1995).
4. F. Diaz-Doutón et al., "Comparison of the retinal image quality with Hartmann-Shack wavefront sensor and a double-pass instrument," *Invest. Ophthalmol. Vis. Sci.* **47**(4), 1710–1716 (2006).
5. P. Artal et al., "An objective scatter index based on double-pass retinal images of a point source to classify cataracts," *PLoS One* **6**, e16823 (2011).
6. A. Guirao et al., "Average optical performance of the human eye as a function of age in a normal population," *Invest. Ophthalmol. Visual Sci.* **40**(1), 203–213 (1999).
7. S. Marcos, E. Moreno, and R. Navarro, "The depth-of-field of the human eye with polychromatic light from objective and subjective measurements," *Vision Res.* **39**(12), 2039–2049 (1999).
8. N. López-Gil, "Estudio de la calidad de la imagen retiniana en relación con el mecanismo de la acomodación," Thesis doctoral, Universidad de Murcia, Spain (1997).
9. M. Aldaba et al., "Measuring the accommodative response with a double-pass system: comparison with the Hartmann-Shack technique," *Vision Res.* **62**, 26–34 (2012).
10. M. Aldaba et al., "Age-related changes in accommodation measured with a double-pass system," *Ophthalmic Physiol. Opt.* **33**(4), 508–515 (2013).
11. J. L. Güell et al., "Optical quality analysis system: instrument for objective clinical evaluation of ocular optical quality," *J. Cataract. Refract. Surg.* **30**(7), 1598–1599 (2004).
12. M. Vilaseca et al., "Optical quality one month after verisyse and Veriflex phakic IOL implantation and Zeiss MEL 80 LASIK for myopia from 5.00 to 16.50 diopters," *J. Refract. Surg.* **25**(8), 689–698 (2009).
13. M. Vilaseca et al., "Effect of laser in situ keratomileusis on vision analyzed using preoperative optical quality," *J. Cataract. Refract. Surg.* **36**(11), 1945–1953 (2010).
14. J. C. Ondategui et al., "Optical quality after myopic photorefractive keratectomy and laser in situ keratomileusis: comparison using a double-pass system," *J. Cataract. Refract. Surg.* **38**(1), 16–27 (2012).
15. J. L. Alio et al., "Comparison of a new refractive multifocal intraocular lens with an inferior segmental near add and a diffractive multifocal intraocular lens," *Ophthalmology* **119**(3), 555–563 (2012).
16. L. S. Seery et al., "Retinal point-spread function after corneal transplantation for Fuchs' dystrophy," *Invest. Ophthalmol. Visual Sci.* **52**(2), 1003–1008 (2011).
17. C. Ortiz et al., "Retinal-image quality and contrast-sensitivity function in age-related macular degeneration," *Curr. Eye Res.* **35**(8), 757–761 (2010).
18. M. Vilaseca et al., "Grading nuclear, cortical and posterior subcapsular cataracts using an objective scatter index measured with a double-pass system," *Br. J. Ophthalmol.* **96**(9), 1204–1210 (2012).
19. A. Benito et al., "Objective optical assessment of tear-film quality dynamics in normal and mildly symptomatic dry eyes," *J. Cataract. Refract. Surg.* **37**(8), 1481–1487 (2011).
20. J. Liang et al., "Objective m of 4 mm measurement of wave aberrations of the human eye with the use of a Hartmann-Shack wave-front sensor," *J. Opt. Soc. Am. A* **11**, 1949–1957 (1994).
21. P. M. Prieto et al., "Analysis of the performance of the Hartmann-Shack sensor in the human eye," *J. Opt. Soc. Am. A* **17**(8), 1388–1398 (2000).
22. F. Sanabria et al., "Spherical refractive correction with an electro-optical liquid lens in a double-pass system," *J. Eur. Opt. Soc. Rapid publ.* **8**, 13062 (2013).
23. H. Hofer et al., "Dynamics of the eye's wave aberration," *J. Opt. Soc. Am. A* **18**, 497–506 (2001).
24. E. Gambra et al., "Accommodative lag and fluctuations when optical aberrations are manipulated," *J. Vision* **9**(6), 1–15 (2009).
25. J. Janesick and T. Elliott, "History and advancement of large array scientific CCD imagers. Astronomical CCD observing and reduction techniques," *Astron. Soc. Pac.* **23**, 1–66 (1992).
26. M. Bigas et al., "Review of CMOS image sensors," *Microelectron. J.* **37**(5), 433–451 (2006).
27. T. Nirmaier, G. Pudasaini, and J. Bille, "Very fast wave-front measurements at the human eye with a custom CMOS-based Hartmann-Shack sensor," *Opt. Express* **11**(21), 2704–2716 (2003).
28. I. Grulkowski et al., "Anterior segment imaging with Spectral OCT system using a high-speed CMOS camera," *Opt. Express* **17**(6), 4842–4858 (2009).

29. Q. Huynh-Thu and M. Ghanbari, "Scope of validity of PSNR in image/video quality assessment," *Electron. Lett.* **44**(13), 800–801 (2008).
30. D. G. Altman and J. M. Bland, "Measurement in medicine: the analysis of method comparison studies," *Statistician* **32**, 307–317 (1983).
31. J. M. Bland and D. G. Altman, "Statistical methods for assessing agreement between two methods of clinical measurement," *Lancet* **327**, 307–310 (1986).
32. D. R. Neal, J. Copland, and D. A. Neal, "Shack–Hartmann wavefront sensor precision and accuracy," *Proc. SPIE* **4779**, 148–160 (2002).
33. J. W. Goodman, "Some fundamental properties of speckle," *J. Opt. Soc. Am.* **66**, 1145–1150 (1976).
34. J. W. Goodman, *Speckle Phenomena in Optics: Theory and Applications*, Roberts and Company Publishers, Colorado (2006).

Ferran Sanabria received his MSc degree in computer science and degree in informatics engineering from the Universitat Politècnica de Catalunya in 1992. He participated in several publicly funded projects and partnership contracts with companies for technology transfer. He is currently working at Centre for Sensors, Instruments & Systems Development (CD6) as a computer engineer and as a researcher in the visual optics group.

Mikel Aldaba Arévalo received a degree in optics and optometry in 2003 from the University of Valladolid (Spain) and a BSc in optometry and vision science in 2005 from the University of Minho (Braga, Portugal). He received a PhD in optical engineering on accommodative response measurement by means of a double-pass system in 2012. He is currently working at Centre for Sensors, Instruments & Systems Development (CD6) as a researcher on visual optics group, focused on accommodation, optical quality, refraction, and aberrometry.

Fernando Díaz-Doutón obtained his BSc degree in physics from the University of Santiago de Compostela (Spain) in 2001. He received his PhD in optical engineering from Universitat Politècnica de Catalunya on 2006. His research work is focused on physiological optics, vision and instrumental optics, and collaborating in the development of biomedical instrumentation for ophthalmology.

Carlos Enrique García-Guerra received the degree in engineering from the Universidad Nacional Autónoma de México (UNAM), Mexico, in 2006 and the joint MSc degree in research on information and communication technologies from the Université Catholique de Louvain (UCL), Belgium, and Universitat Politècnica de Catalunya (UPC), Spain, in 2010. He is currently working towards the joint PhD degree at the Centre for Sensors, Instruments and Systems Development (CD6-UPC), Spain, and Karlsruhe Institute of Technology (KIT), Germany.

Jaume Pujol Ramo received his MSc and PhD degrees in physics from the Universitat Autònoma de Barcelona. In 1984, he joined the Universitat Politècnica de Catalunya, where he is a professor. He is author of over 60 papers, 4 books in physiological optics and color and 8 patents. His main current research interest is the evaluation of the optical quality of the eye and color technology and imaging.